

Chemical and structural investigation of the role of both Mn and Mn oxide in the formation of manganese silicate barrier layers on SiO₂

Cite as: J. Appl. Phys. **110**, 054507 (2011); <https://doi.org/10.1063/1.3630123>

Submitted: 14 June 2011 . Accepted: 25 July 2011 . Published Online: 07 September 2011

P. Casey, J. Bogan, J. G. Lozano, P. D. Nellist, G. Hughes, et al.



View Online



Export Citation

ARTICLES YOU MAY BE INTERESTED IN

[Synchrotron radiation photoemission study of in situ manganese silicate formation on for barrier layer applications](#)

Applied Physics Letters **98**, 113508 (2011); <https://doi.org/10.1063/1.3567926>

[Chemical and structural investigations of the interactions of Cu with MnSiO₃ diffusion barrier layers](#)

Journal of Applied Physics **112**, 064507 (2012); <https://doi.org/10.1063/1.4752874>

[Self-forming diffusion barrier layer in Cu–Mn alloy metallization](#)

Applied Physics Letters **87**, 041911 (2005); <https://doi.org/10.1063/1.1993759>

HIDEN
ANALYTICAL

Instruments for Advanced Science

- Knowledge,
- Experience,
- Expertise

[Click to view our product catalogue](#)

Contact Hiden Analytical for further details:

www.HidenAnalytical.com
info@hiden.co.uk



Gas Analysis

- dynamic measurement of reaction gas streams
- catalysis and thermal analysis
- molecular beam studies
- dissolved species probes
- fermentation, environmental and ecological studies



Surface Science

- UHVTPD
- SIMS
- end point detection in ion beam etch
- elemental imaging - surface mapping



Plasma Diagnostics

- plasma source characterization
- etch and deposition process reaction kinetic studies
- analysis of neutral and radical species



Vacuum Analysis

- partial pressure measurement and control of process gases
- reactive sputter process control
- vacuum diagnostics
- vacuum coating process monitoring

Chemical and structural investigation of the role of both Mn and Mn oxide in the formation of manganese silicate barrier layers on SiO₂

P. Casey,^{1,a)} J. Bogan,¹ J. G. Lozano,² P. D. Nellist,² and G. Hughes¹

¹*School of Physical Sciences, Dublin City University, Glasnevin, Dublin 9, Ireland*

²*Department of Materials, University of Oxford, Parks Road, Oxford OX1 3PH, United Kingdom*

(Received 14 June 2011; accepted 25 July 2011; published online 7 September 2011)

In this study, Mn silicate (MnSiO₃) barrier layers were formed on thermally grown SiO₂ using both metallic Mn and oxidized Mn films, in order to investigate the role of oxygen in determining the extent of the interaction between the deposited Mn and the SiO₂ substrate. Using x-ray photoelectron spectroscopy, it has been shown that a metallic Mn film with an approximate thickness of 1 nm cannot be fully converted to Mn silicate following vacuum annealing to 500 °C. Transmission electron microscopy (TEM) analysis suggests the maximum MnSiO₃ layer thickness obtainable using metallic Mn is ~1.7 nm. In contrast, a ~1 nm partially oxidized Mn film can be fully converted to Mn silicate following thermal annealing to 400 °C, forming a MnSiO₃ layer with a measured thickness of 2.6 nm. TEM analysis also clearly shows that MnSiO₃ growth results in a corresponding reduction in the SiO₂ layer thickness. It has also been shown that a fully oxidized Mn oxide thin film can be converted to Mn silicate, in the absence of metallic Mn. Based on these results it is suggested that the presence of Mn oxide species at the Mn/SiO₂ interface facilitates the conversion of SiO₂ to MnSiO₃, in agreement with previously published studies. © 2011 American Institute of Physics. [doi:10.1063/1.3630123]

INTRODUCTION

Copper has now replaced aluminum as the metal of choice for interconnects in microelectronic devices, due to its lower resistivity and increased resistance to electromigration.^{1,2} However, studies have shown that a physical barrier is required to surround the Cu interconnect and prevent both the diffusion of Cu into the insulating SiO₂ based dielectric materials, and the diffusion of O and H₂O into the Cu.³ Self forming diffusion barrier layers have been proposed as a scalable alternative to Ta/TaN barrier layers for future interconnect generations.² Both manganese silicate and manganese oxide barrier layers have been the subject of considerable study due to favorable alloying properties⁴ and improved copper adhesion compared to other barrier layer candidates such as TaN.¹ In a recent high resolution photoemission study, Casey *et al.*⁵ have shown that Mn silicate (MnSiO₃) layers, free from Mn oxide, can be formed through ultra high vacuum (UHV) annealing of metallic Mn on thermally grown SiO₂ surfaces. However, it was also shown that this Mn silicate growth method is self limiting at high temperature, with the maximum thickness of the MnSiO₃ layer calculated to be approximately 2 nm, resulting in the presence of residual metallic Mn on the surface following annealing. Previous studies⁶ have shown that unreacted metallic Mn remaining after barrier layer formation can diffuse to the surface of the deposited Cu interconnect during high temperature annealing and can be subsequently removed using an oxidation process. However, it has also been suggested that the presence of Mn within Cu during thermal annealing restricts Cu grain growth, leading to

an increase in the final resistance of the interconnect.^{1,6} Therefore, it would be preferable if the Mn silicate growth reaction could be controlled more accurately in order to determine the thickness of the MnSiO₃ layer and prevent the presence of residual metallic Mn.

Ablett *et al.*⁷ have previously discussed the factors which determine the initial stages of Mn silicate growth on silica based dielectrics. It was suggested that absorbed water on dielectric surfaces leads to the presence of -OH groups, which interact with deposited Mn to form Mn oxide, with these Mn oxide species in turn reacting with silicon in the SiO₂ to form MnSiO₃. It has also been suggested that the absence of absorbed water species on thermally grown SiO₂ layers reduces Mn oxide formation, hence limiting the maximum thickness of Mn silicate layers which can be formed on the surface. However, the precise role of SiO₂, metallic Mn and Mn oxide species within the Mn silicate formation process has not been investigated experimentally. Therefore, the focus of this study is to determine if the thickness of MnSiO₃ barrier layers grown on thermally grown SiO₂ surfaces is limited by the presence of additional oxygen species, beyond that found within the SiO₂ layer.

The chemical interactions between metallic Mn, partially oxidized Mn and fully oxidized Mn thin films on thermally grown SiO₂ were systematically investigated using *in situ* x-ray photoelectron spectroscopy (XPS). The formation of Mn oxide species on the surface of dielectric materials through the presence of surface -OH groups, as described by Ablett *et al.*,⁷ would be very difficult to control experimentally. Therefore, the experimental approach adopted in this study was to form partially oxidized and fully oxidized Mn thin films in UHV conditions through the evaporation of metallic Mn in a controlled oxygen background pressure. Also,

^{a)}Author to whom correspondence should be addressed. Electronic mail: patrick.casey8@mail.dcu.ie.

given that barrier layer formation and XPS analysis was performed fully *in situ* in the UHV analysis system, this allowed the role of both oxidized and metallic species to be investigated without the complicating influence of ambient oxidation effects. Following the completion of XPS analysis, a protective copper capping layer (20–30 nm) was deposited on selected samples before they were removed from vacuum and subsequently analyzed by transmission electron microscopy (TEM), in order to accurately determine the thickness and uniformity of the MnSiO₃ layers.

EXPERIMENTAL DETAILS

High quality thermally grown SiO₂ layers on silicon, with a thickness of 5.4 nm, were grown using the Semitool dry oxidation process in a Thermoco 9002 series furnace at 850 °C. The thickness of the thermal oxide was chosen so that the Si substrate (Si⁰) and SiO₂ component peaks of the Si 2p core level profile could be observed throughout all experimental stages. This allowed the extent of SiO₂ to MnSiO₃ conversion to be approximated by expressing the integrated area of the MnSiO₃ component peak as a percentage of the SiO₂ component peak area. The SiO₂ surfaces were prepared using a standard degreasing procedure of successive dips in acetone, methanol and isopropyl alcohol before being loaded into a UHV deposition and analysis system. Samples were then degassed at ~200 °C for 2 hs, with the UHV chamber reaching a maximum pressure of 5×10^{-9} mbar during degassing. The XPS analysis was carried out using a VG Microtech electron spectrometer at a base pressure of 1×10^{-9} mbar. The photoelectrons were excited with a conventional Mg K α ($h\nu = 1253.6$ eV) x-ray source and an electron energy analyzer operating at a 20 eV pass energy, yielding an overall resolution of 1.2 eV. High temperature annealing studies were carried out in vacuum at a pressure of 5×10^{-9} mbar, with samples kept at the target temperature for 60 mins. Hydrochloric acid etched Mn chips, with a purity of ~99.9%, were used as a source material for the deposition of oxygen free metallic Mn thin films using electron beam evaporation. Metallic manganese thin film deposition was performed at elevated substrate temperature (150 °C) using an Oxford Applied Research EGC04 mini electron-beam evaporator, at a chamber pressure of 5×10^{-9} mbar. The deposition of both partially and fully oxidized Mn films was carried out by the controlled introduction of O₂ gas into the UHV chamber during metallic Mn deposition. The XPS core level spectra were curve fitted using Voigt profiles composed of Gaussian and Lorentzian line shapes in a 3:1 ratio and using a Shirley-type background. The full width at half maximum (FWHM) of the Si 2p bulk peak was 0.9 eV, with SiO₂ and Mn silicate component peaks in the range 1.1 to 1.2 eV. The FWHM of the O 1s SiO₂ component was 1.2 eV with Mn silicate and Mn oxide peaks in the range of 1.2 to 1.1 eV.

It should be noted that curve fitting of the Mn 2p spectrum could not be performed given that XPS ghost peaks⁸ emanating from the Mn 2p^{1/2} are present within the peak profile of the Mn 2p^{3/2} component. As such, only non-curve fitted Mn 2p spectra are included in this study. The Mn 2p spectra are primarily used to identify the presence of metallic

Mn and oxidized Mn species on the sample surface as these component peaks are easily identified from the Mn 2p^{3/2} peak profile without curve fitting. However, Mn 2p spectra could not be used to conclusively identify the presence of differing oxidized Mn species such as Mn silicate and Mn oxide, therefore these chemical species are identified in this study using curve fitted O 1s and Si 2p spectra.

High resolution transmission electron microscopy (HRTEM) studies were performed using a JEOL-JEM 3000 F and JEOL-JEM 4000EX electron microscopes operating at 300 and 400 kV, respectively. Samples in cross section geometry were prepared by the conventional method of grinding and polishing followed by Ar⁺ milling in a Gatan PIPS until electron transparent. The HRTEM micrographs were calibrated using the silicon (111) planes spacing as a reference.

EXPERIMENTAL RESULTS AND DISCUSSION

Curve fitted O 1s and Si 2p core level spectra taken from the 5.4 nm thermal SiO₂ surface are shown in Fig. 1. The corresponding spectra taken following the deposition of a ~1 nm metallic Mn thin film onto the SiO₂ surface at elevated substrate temperature (150 °C) are also shown in Fig. 1. Curve fitting analysis shows small changes to the core levels profiles suggesting that Mn deposition resulted in the growth of additional component peaks in both the O 1s and Si 2p spectra separated from the SiO₂ components by 1.4 and 1.3 eV, respectively. These peaks are attributed to the presence of the Mn silicate species MnSiO₃, in agreement with previous photoemission results.⁵ A series of high temperature vacuum anneals between 300 °C and 500 °C were then performed on the sample. The spectra in Fig. 1 show evidence for further Mn silicate formation following these anneals, and this is supported by changes in the Mn 2p spectrum in Fig. 2 which show the growth of an oxidized Mn component peak on the higher binding energy side of the

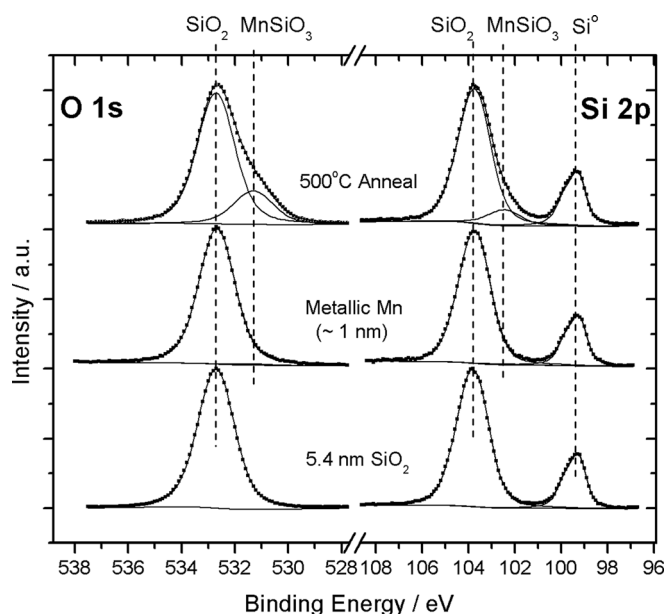


FIG. 1. Curve fitted O 1s and Si 2p spectra showing the growth of Mn silicate (MnSiO₃) following the deposition of metallic Mn (~1 nm) onto SiO₂ thermal oxide surface and subsequent UHV annealing.

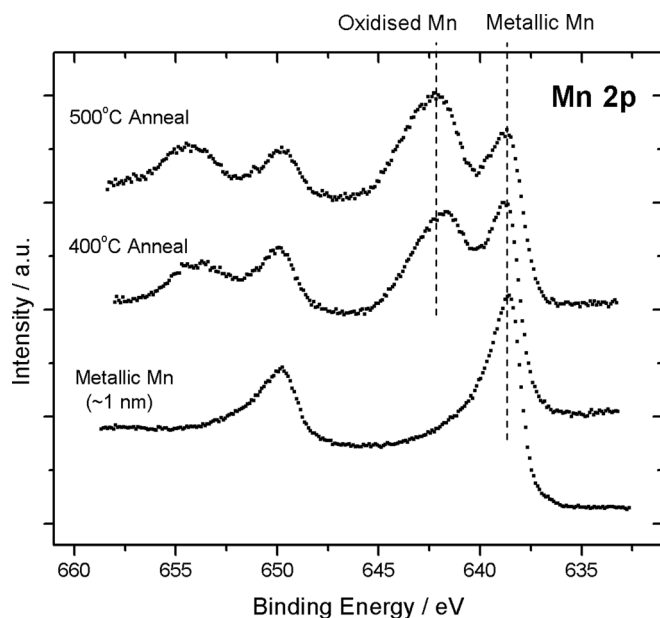


FIG. 2. Mn 2p spectra, corresponding to Fig. 1, show the presence of residual metallic Mn on the surface following 500 °C annealing. This result suggests that the interaction of metallic Mn and SiO₂ is self limiting at high temperature.

metallic Mn peak.⁹ The presence of residual metallic Mn following the 500 °C anneal suggests that the interaction of metallic Mn with SiO₂ is self limiting at this temperature, in agreement with previous results.^{5,7} Rudimentary peak fitting (not shown) of the Mn 2p spectra in Fig. 2 suggests that only ~0.5 nm of the deposited Mn film was converted to Mn silicate following the 500 °C anneal. This limited scale of Mn silicate growth can also be seen from the corresponding Si 2p spectrum which shows that only ~12% of the SiO₂ component peak was converted to Mn silicate. The results shown in Figs. 1 and 2 suggest that the thickness of manganese silicate barrier layers formed through the deposition of purely metallic Mn is self limiting at high temperature. Based on photoemission thickness calculations¹⁰ the limiting thickness of the MnSiO₃ was calculated to be approximately 2 nm following the 500 °C vacuum anneal. It should be noted that while the SiO₂ surfaces used in this study were degassed prior to Mn deposition at a temperature of ~200 °C for 2 hs, the work of Proost *et al.*¹¹ suggests that this may not have been sufficient to remove all of the chemisorbed water present on the surface. As stated previously, Ablett *et al.*⁷ have suggested that the interaction of metallic Mn and adsorbed water on silica surfaces may promote the growth of Mn oxide species, with these Mn oxide species subsequently reacting with SiO₂ to form Mn silicate. Therefore, it is suggested that the presence of chemisorbed water may have contributed to the partial conversion of metallic Mn to Mn silicate seen in Figs. 1 and 2. However, this has not been shown conclusively in this study.

In order to determine if the chemical reactivity of metallic Mn on SiO₂ surfaces is limited by the presence of additional oxygen species, specifically in the form of Mn oxide, a partially oxidized Mn film was deposited onto the SiO₂ surfaces and annealed to high temperature. Figure 3 shows

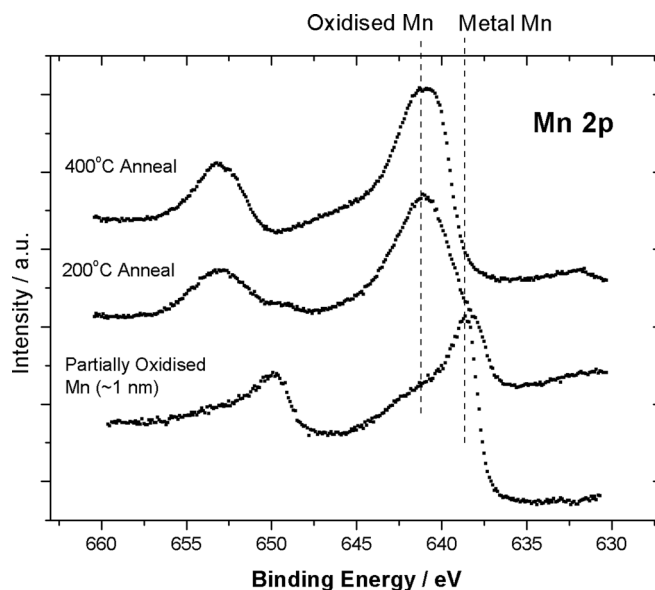


FIG. 3. Mn 2p spectra taken following the deposition of partially oxidized Mn (~1 nm) onto SiO₂ show the presence of both metallic Mn and oxidized Mn component peaks. Spectra taken following 400 °C annealing show the complete conversion of metallic Mn to Mn silicate.

Mn 2p spectra taken following the deposition of metallic Mn in an O₂ partial pressure of 5×10^{-8} mbar onto the SiO₂ surface at elevated substrate temperature (150 °C), leading to an O₂ exposure of ~30 Langmuir (L). The Mn 2p spectrum clearly shows the presence of both metallic Mn and oxidized Mn spectral components, with curve fitting analysis suggesting a metallic Mn:oxidized Mn ratio of 5:1. Angular resolved Mn 2p spectra (not shown) indicate no evidence for spatial segregation between the oxidized and metallic species, which suggests that the oxygen content is homogeneously distributed throughout the deposited film. While detailed chemical analysis of Mn species cannot be achieved by curve fitting the Mn 2p spectrum as mentioned previously, the curve fitted O 1s and Si 2p spectra in Fig. 4 can be used to determine the chemical species present on the SiO₂ surface following deposition of the partially oxidized Mn film. It can be seen from Fig. 4 that O 1s spectra show the presence of two additional component peaks on the lower binding energy (LBE) side of the SiO₂ component following deposition. The peak at 531.3 eV is again attributed to the presence of Mn silicate which formed upon deposition, which is confirmed by the growth of a Mn silicate component peak in the corresponding Si 2p spectrum at 102.6 eV (Fig. 4). In addition to this, the O 1s spectrum also shows evidence for a third component peak at a binding energy position of 530.0 eV, which is attributed to the presence of Mn oxide in agreement with previous studies.¹² The formation of Mn oxide species following ~30 L O₂ exposure is in agreement with the work of Lescop¹³ who has shown that the oxidation of Mn can occur at oxygen exposure levels less than 20 L. Based on this analysis, it is apparent that the chemical species present on the surface prior to high temperature annealing are metallic Mn, Mn oxide, Mn silicate, and SiO₂. The sample was subsequently annealed to a maximum temperature of 400 °C in UHV and the corresponding photoemission spectra are also

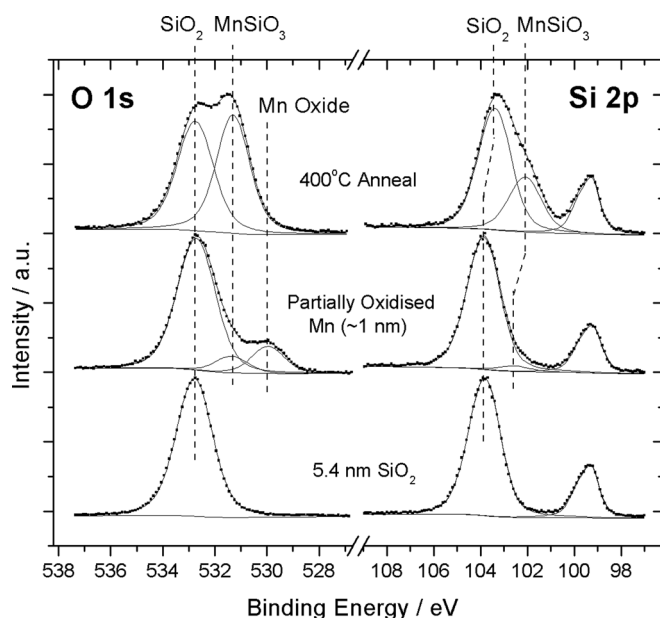


FIG. 4. Curve fitted O 1s and Si 2p spectra corresponding to Fig. 3. Spectra show the complete conversion of both metallic Mn and Mn oxide to form MnSiO₃, resulting in higher levels of silicate growth than that seen in Fig. 1 which indicates the increased reactivity of partially oxidized Mn films on SiO₂.

shown in Figs. 3 and 4. It can be seen from Fig. 4 that annealing to 400 °C has resulted in considerable growth of Mn silicate, as evidenced by growth of the MnSiO₃ component peaks in both the O 1s and Si 2p spectra. Curve fitting of the Si 2p spectrum following annealing suggests that 48% of the SiO₂ component peak was converted to Mn silicate, which is a considerably larger value than that seen following the deposition of metallic Mn in Fig. 1. XPS thickness calculations¹⁰ suggest that the thickness of this silicate layer is ~3 nm. It is suggested that this increased thickness may be attributed to an increase in the chemical reactivity of the partially oxidized Mn species on SiO₂, compared to that of the purely metallic Mn film. This increased chemical reactivity of the partially oxidized Mn film is also shown by the Mn 2p spectra in Fig. 3 which show no evidence for the presence of residual metallic Mn following 400 °C annealing, again in contrast to the results seen following the deposition of metallic Mn in Fig. 2.

Figure 5 shows HRTEM images taken from the 5.4 nm thermal SiO₂ surface [Fig. 5(a)], as well as images taken following the growth of barrier layers using partially oxidized Mn [Fig. 5(b)] and metallic Mn [Fig. 5(c)]. The images are used to more accurately quantify the thickness of the barriers formed on both samples, and as such offer further evidence for the increased chemical reactivity of partially oxidized Mn. The HRTEM measured thickness values in Table I indicate that the thickness of the barrier layer formed using purely metallic Mn is 1.7 nm [Fig. 5(c)], while the Mn silicate layer formed using partially oxidized Mn is measured to be 2.6 nm [Fig. 5(b)]. It should be noted that the TEM thickness values shown in Table I are in close agreement with the corresponding values calculated using XPS, suggesting the photoemission calculations used in this study are accurate. It should also be noted that XPS thickness calcula-

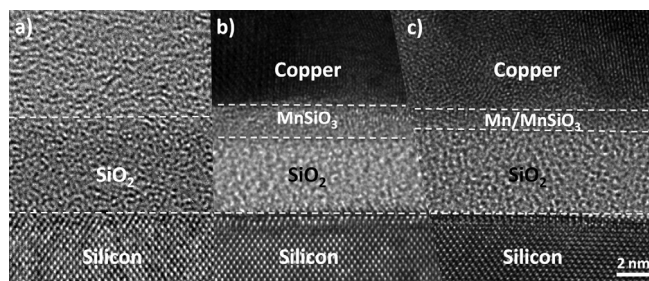


FIG. 5. HRTEM images taken from the as grown SiO₂ thermal oxide (a), the barrier layer formed using partially oxidized Mn (b), and the barrier layer formed using metallic Mn (c). Images clearly show that the MnSiO₃ layer formed using partially oxidized Mn is considerably thicker than that formed using metallic Mn. It can also be seen that MnSiO₃ growth has resulted in a corresponding reduction in SiO₂ thickness, indicating the conversion of SiO₂ to MnSiO₃ during barrier layer formation.

tions suggest that the deposited thickness of Mn in both films was the same (~1 nm). Therefore, the increased thickness of the Mn silicate layer shown in Fig. 5(b) is attributed to an increase in the chemical reactivity of the partially oxidized Mn film compared to that of the purely metallic Mn film.

It should also be noted that while the partially oxidized Mn film consisted of ~15% oxidized Mn, the remaining oxygen required to form the fully oxidized MnSiO₃ layer must come from the conversion of SiO₂ to Mn silicate, given that all experimental stages were carried out in UHV. The conversion of SiO₂ to MnSiO₃ during barrier layer growth is confirmed by the HRTEM images in Fig. 5 which clearly show that the increased barrier layer thickness seen in Fig. 5(b) results in a corresponding reduction in the thickness of the underlying SiO₂. This observation is analogous to a comparable study by Copel *et al.*¹⁴ who investigated the interaction of La₂O₃ films on SiO₂ surfaces and reported that the growth of La silicate through thermal annealing resulted in a corresponding reduction in SiO₂ thickness. The reduction of SiO₂ thickness during the conversion of SiO₂ to MnSiO₃ is quantified in Table I, with TEM thickness values suggesting that the presence of Mn oxide species within the partially oxidized film allowed for increased levels of SiO₂ conversion. Therefore, it is suggested that the presence of Mn oxide allows Mn silicate layers of increased thickness to be formed by facilitating the conversion of both SiO₂ and Mn to MnSiO₃. Based on these results it can be stated that the presence of additional oxygen within a metallic Mn film is essential in order to form Mn silicate films with a thickness greater than ~2 nm on thermally grown SiO₂.

It should be noted that the shift to LBE seen in the SiO₂ component of the Si 2p spectra in Fig. 4 is attributed to the thinning of the SiO₂ layer following Mn silicate growth. It

TABLE I. HRTEM thickness values corresponding to the images shown in Fig. 5.

	SiO ₂ thickness (nm)	Mn barrier layer thickness (nm)
Thermally grown SiO ₂ (5a)	5.4	–
Partially oxidized Mn (5b)	4.1	2.6
Metallic Mn (5c)	4.5	1.7

has been shown by Iwata *et al.*¹⁵ that the binding energy (BE) separation between the Si⁰ and SiO₂ components of the Si 2p profile may be increased as a function of increasing SiO₂ thickness, due to the buildup of surface electronic charge during the photoemission process. In agreement with this, curve fitting techniques suggest that the Si⁰-SiO₂ BE separation is reduced from an initial value of 4.4 eV for the 5.4 nm SiO₂ surface to a value of 4.0 eV following the growth of Mn silicate and corresponding reduction in SiO₂ thickness. The effects of surface charging are accommodated for during the peak fitting process by linking the B.E. position of the Mn silicate component to that of the SiO₂ component, using a BE separation of 1.4 eV in agreement with previous studies.⁵

Along with the conversion of metallic Mn, the O 1s spectra in Fig. 4 also show evidence for the complete conversion of Mn oxide to Mn silicate following high temperature annealing. This result indicates that MnSiO₃ layers free from metallic Mn and Mn oxide can be formed by the thermal annealing of partially oxidized Mn on SiO₂ surfaces. The conversion of Mn oxide to Mn silicate is in contrast to the finding of Gordon *et al.*^{1,3} who have suggested that Mn oxide is unreactive on SiO₂ surfaces. However, the chemical reactivity of Mn oxide species within a metallic Mn matrix may be different to that of fully oxidized Mn oxide films. Therefore, a metal free Mn oxide layer, with a thickness of ~1 nm, was deposited in order to determine the chemical stability of fully oxidized Mn on SiO₂. The fully oxidized Mn film was formed by evaporation of metallic Mn in an O₂ oxygen background pressure of 1×10^{-7} mbar at elevated substrate temperature of 150 °C. A post deposition anneal at the same temperature and O₂ background pressure was then performed leading to a total O₂ exposure of ~400 L. The Mn 2p spectrum taken following post-deposition annealing (not shown) displays no evidence for the presence of metallic Mn on the surface, showing that the film is fully oxidized. The corresponding O 1s spectrum in Fig. 6 shows the presence of a Mn oxide component at a binding energy position of 530.2 eV, which is close to that previously attributed to the Mn oxide species MnO.¹² Given the difficulty in curve fitting Mn 2p spectra obtained using conventional non-monochromated XPS, the exact stoichiometry of the Mn oxide species deposited in this study cannot be established. However, it can be clearly stated that the film is fully oxidized and free from metallic Mn.

A series of high temperature vacuum anneals between 300 °C and 500 °C were then performed on the sample. In agreement with the results of the partially oxidized Mn film, it can be seen from both the O 1s and Si 2p spectra in Fig. 6 that high temperature annealing results in the conversion of Mn oxide to Mn silicate. Given that there is no evidence for the presence of metallic Mn on the surface of this sample, this experimental result shows that fully oxidized Mn can also be converted to Mn silicate following high temperature annealing on SiO₂ surfaces. This result is in agreement with recent publications^{16,17} which have reported that Mn oxide layers formed on SiO₂ surface using chemical vapor deposition can be converted to Mn silicate following thermal annealing. In addition to this, it has also been shown that other metal oxide species such as La₂O₃¹⁴ and MgO_x¹⁸ can be converted to

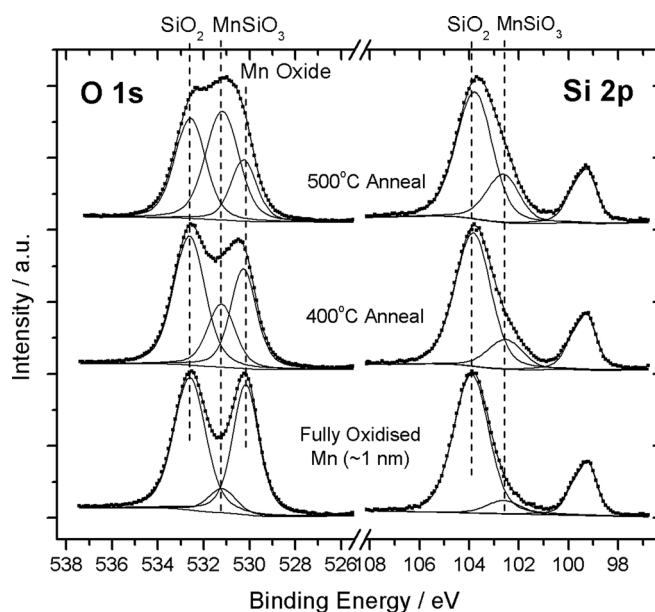


FIG. 6. Curve fitted O 1s and Si 2p spectra taken following the deposition of a fully oxidized Mn oxide layer (~1 nm) and subsequent UHV annealing, showing the conversion of Mn oxide to Mn silicate. Spectra taken from the 5.4 nm SiO₂ surface prior to Mn oxide deposition are not shown, but are identical to those shown in Figs. 1 and 4.

metal silicate species following thermal annealing on SiO₂ surfaces. The scale of Mn silicate growth is again quantified using curve fitting techniques, with the Si 2p spectra in Fig. 6 showing that 36% of the SiO₂ component peak being converted to Mn silicate. It should be noted that the SiO₂ component of the Si 2p spectrum in Fig. 6 does not show the same shift to LBE previously observed in Fig. 4 following the reduction of SiO₂ thickness, and the corresponding reduction of surface electronic charging effects. It is suggested that these charging effects were not reduced to the same extent in Fig. 6, given that lower levels of SiO₂ conversion to MnSiO₃ were observed in this sample. Also, the presence of Mn oxide species, with comparatively high resistivity, on the SiO₂ surface in Fig. 6 may have also increased the level of photoemission surface charging effects compared to that seen in Fig. 4.

Further experiments (not shown) involving the deposition of partially oxidized Mn films of greater thickness (>1.5 nm) were also carried out in order to determine if the deposited film thickness is also a limiting factor in Mn silicate growth. Spectra taken after 500 °C annealing showed evidence for greater levels of Mn silicate growth than that seen in Figs. 3 and 4, however, there was also evidence for the presence of residual metallic Mn which had not been converted to Mn silicate at this temperature. Therefore, based on the results of this study it is suggested that even when sufficient levels of Mn oxide are present on the surface the thickness of Mn silicate layers formed on SiO₂ is still self limiting at high temperature.

CONCLUSIONS

The results of this study show that the growth of Mn silicate barrier layers on SiO₂ surfaces is self limited by the

availability of additional oxygen, beyond that which is present within the SiO₂ layer. It has been shown that a ~1 nm metallic Mn film cannot be fully converted to Mn silicate following 500 °C annealing. As a result, Mn silicate layers with a thickness greater than 1.7 nm cannot be formed following the deposition of purely metallic Mn and subsequent UHV annealing on a thermally grown SiO₂ layer. It has also been shown that a partially oxidized Mn film of similar thickness (~1 nm), containing approximately 15% Mn oxide, can be fully converted to form a Mn silicate layer of greater thickness (2.6 nm) which is free from metallic Mn and Mn oxide. HRTEM images taken from these samples show that MnSiO₃ growth causes a corresponding reduction in the SiO₂ layer thickness. This result is attributed to the conversion of SiO₂ to Mn silicate during UHV annealing and suggests that while the presence of Mn oxide is required to achieve full conversion of 1 nm Mn films to Mn silicate, the remaining oxygen required for silicate growth can be obtained from the SiO₂ film. Therefore, only low levels of additional oxygen are required to increase film reactivity. This may be of relevance for the practical implementation of MnSiO₃ barrier layer formation processes in device fabrication, given that the integration of excess oxygen into the Mn layer may decrease the reportedly high diffusivity of metallic Mn within Cu layers,⁷ one of the main factors which has led to the investigation of Mn based barrier layers for Cu interconnects. It has also been shown in this study that fully oxidized Mn films, free from metallic Mn, can be converted to Mn silicate using thermal annealing on SiO₂ surfaces. Given that conformal deposition techniques such as atomic layer deposition are more suited to the deposition of metal oxide species than contaminant free metallic films, the use of fully or partially oxidized Mn films may offer a route to integrate Mn silicate structures into ultrathin barrier layer formation. However, it should be noted that the chemical reactivity of

Mn oxide films on SiO₂ may depend greatly on factors such as oxide stoichiometry and film deposition method.

ACKNOWLEDGMENTS

The authors would like to gratefully acknowledge financial support from the SFI PI program under Grant No. 08/IN.1/I2052. J.G. Lozano would like to acknowledge the support of the European Commission under the Marie Curie Programme 2009. The authors would also like to thank the Tyndall National Institute in Cork, Ireland for SiO₂ thermal oxide fabrication.

¹R. Gordon, H. Kim, International Patent No. WO 2009/117670 A2, 24 Sept. (2009).

²Y. Lee and Y.-L. Kuo, *JOM* **59**, 44 (2007).

³Y. Au, Y. Lin, H. Kim, E. Beh, Y. Liu, and R. G. Gordon, *J. Electrochem. Soc.* **157**, D 341 (2010).

⁴J. Koike and M. Wada, *Appl. Phys. Lett.* **87**, 041911 (2005).

⁵P. Casey, J. Bogan, B. Brennan, and G. Hughes, *Appl. Phys. Lett.* **98**, 113508 (2011).

⁶J. Iijima, Y. Fujii, K. Neishi, and J. Koike, *J. Vac. Sci. Technol. B* **27**, 1963 (2009).

⁷J. M. Ablett, J. C. Woicik, Z. Tokei, S. List, and E. Dimasi, *Appl. Phys. Lett.* **94**, 042112 (2009).

⁸M. O. Krause and J. G. Ferreira, *J. Phys. B: At. Mol. Phys.* **8**, 12 (1975).

⁹U. Manju, D. Topwal, G. Rossi, and I. Vobornik, *Phys. Rev. B* **82**, 035442 (2010).

¹⁰M. P. Seah and S. J. Spencer, *Surf. Interface Anal.* **33**, 640 (2002).

¹¹J. Proost, E. Kondoh, G. Vereecke, M. Heyns, and K. Maex, *J. Vac. Sci. Technol., B* **16**, 2091 (1998).

¹²A. A. Audi and P. M. A. Sherwood, *Surf. Interface Anal.* **33**, 274 (2002).

¹³B. Lescop, *Appl. Surf. Sci.* **252**, 2276 (2006).

¹⁴M. Copel, E. Cartier, and F. M. Ross, *Appl. Phys. Lett.* **78**, 1607 (2001).

¹⁵S. Iwata and A. Ishizaka, *J. Appl. Phys.* **79**, 6653 (1996).

¹⁶N. M. Phuong, K. Matsumoto, K. Maekawa, and J. Koike, Abstracts of Papers, Materials Research Society Spring Meeting, San Francisco Abstract O6.4 (2011).

¹⁷V. K. Dixit, K. Neishi, N. Akao, and J. Koike, *IEEE Trans. Device Mater. Reliab.* **11**, 295 (2011).

¹⁸P. Casey and G. Hughes, *J. Appl. Phys.* **107**, 074107 (2010).